

The Siemens logo is displayed in a bold, teal, sans-serif font. It is positioned in the upper left corner of the page, above the tagline. The background of the entire page is a close-up photograph of several cylindrical electromagnetic components, likely solenoids or relays, with copper windings and dark grey or black casings. The lighting is dramatic, highlighting the metallic textures and the intricate details of the components.

**SIEMENS**

*Ingenuity for life*

Siemens Digital Industries Software

# Effects of incorporating hysteresis in the simulation of electromagnetic devices

## Executive summary

Hysteresis modelling in Simcenter MAGNET™ v7.9 software enables engineers and scientists to model a real-world scenario by incorporating the effects of iron losses in the simulation of low-frequency electromagnetic devices. The accurate representation of a ferromagnetic material by the complete BH loop instead of the SV BH curve affects the local quantities, i.e., magnetic field distributions. As a result, the operating point of the device and other global quantities, such as input power, torque/force, etc. also change and this can be critical for the multi-objective optimization of the device to find the best design. The incorporation of hysteresis is also a crucial step-forward towards the accurate modelling of these materials in multi-physics simulations of electromagnetic devices in the Simcenter® environment where the magnetic properties of these materials are also affected by mechanical stresses and high temperatures.

Sajid Hussain and Kang Chang

[siemens.com/simcenter](https://www.siemens.com/simcenter)

# Introduction

The finite element (FE) method is widely used in commercial computer-aided design (CAD) software industry to analyze and design low-frequency electromagnetic devices, such as actuators, motors and transformers. Maxwell's equations are discretized to compute magnetic fields in complex geometries which would not be possible to simulate otherwise. Advanced numerical techniques have been developed to improve the accuracy of the solutions for the better prediction of the performance of these electromagnetic devices. However, field solutions will not be accurate if magnetic properties of the ferromagnetic materials, with which these devices are manufactured, are not properly modelled in CAD simulations.

In commercial software, magnetic properties of ferromagnetic materials are typically modelled by a nonlinear single-valued (SV) magnetization curve (known as the BH curve, an example is shown in figure 1) for various reasons including numerical stability, the limited computational resources available and the lack of material data. Such an approximation leads to magnetic lossless simulations which means that global results, e.g., the torque of the motor, do not include any magnetic (iron) losses. These are later computed in a post-processing stage often with empirical loss formulae developed in the early 20<sup>th</sup> century. The following equation (1) represents the energy balance in this scenario.

$$(1) \quad E_{input} = E_{output} + E_{ohmic} + E_{StoredMag}$$

The  $E_{ohmic}$  and  $E_{StoredMag}$  terms in (1) are the ohmic ( $I^2R$ ) loss and the stored magnetic energy in the material, respectively. Note that there is no iron loss term in (1) which means that the SV simulations do not incorporate iron loss in the field solutions.

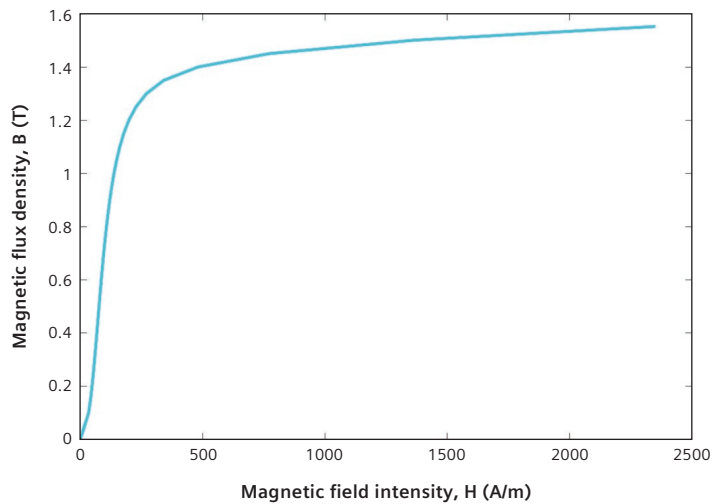


Figure 1: Single-valued BH curve of 35WW300 non-oriented electrical steel.

# Incorporating hysteresis

In reality, ferromagnetic materials do not exhibit a SV BH curve but a BH loop (like the one shown in figure 2). Energy is dissipated inside the material in the form of heat when the applied magnetic field intensity  $H$  changes. The loss as a result of this is called the hysteresis loss. The inclusion of hysteresis in the FE simulation modifies the energy balance equation (1) as shown below.

$$(2) \quad E_{input} = E_{output} + E_{ohmic} + E_{hys}$$

The  $E_{hys}$  term in (2) represents both hysteresis loss and stored magnetic energy in the ferromagnetic material. For this reason, the stored magnetic energy and coenergy tab in Simcenter MAGNET v7.9 is disabled for hysteresis simulations. This is demonstrated in detail in the single sheet tester (SST) sample example in the next section.

Despite the advent of powerful computers and advanced numerical techniques, the inclusion of hysteresis in commercial software remains a rare practice. Although academic research has produced many hysteresis models, such as the Jiles-Atherton [1] and the Preisach [2] models, commercial FE software companies have not generally adopted them for accurately representing the magnetic behaviour of ferromagnetic materials in the simulation of modern electromagnetic devices, e.g., actuators, magnetic storage and recording devices, power transformers, variable speed electric motors, etc. Now that the simulation times have been reduced (as a result of faster processors), computationally expensive hysteresis models can be employed at a large scale in complex geometries of these devices.

Simcenter MAGNET by Siemens Digital Industries Software is a general-purpose 2D/3D electromagnetic field simulation software used for the virtual prototyping of simple to complex electromagnetic and electromechanical devices. Using Simcenter MAGNET, engineers and scientists can design motors, sensors, transformers, actuators, solenoids or any component with permanent magnets or coils thus saving both time and money.

This paper focuses on the application of a new advanced feature of Simcenter MAGNET v7.9 which allows users to incorporate hysteresis in the field solutions using the vector Jiles-Atherton hysteresis (Hys) model [3]. The feature can be enabled when the simulation is solved using the Transient solver in 2D (with and without motion).

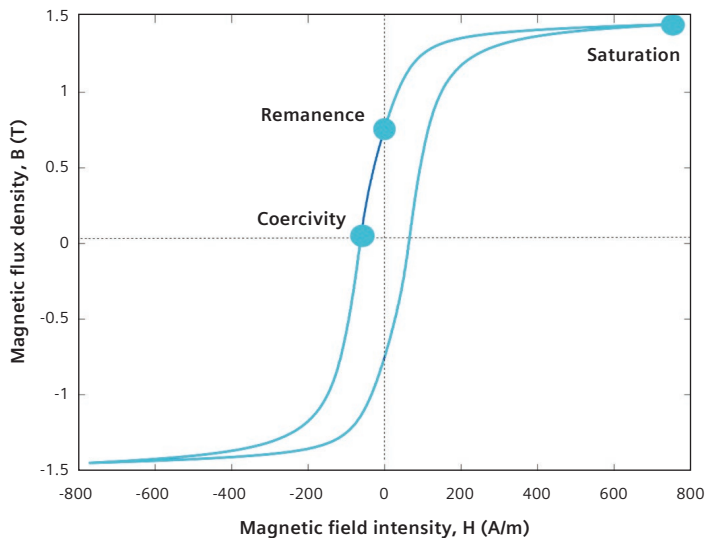


Figure 2: BH loop of 35WW300 non-oriented electrical steel.

# Application examples

In this section, we will discuss the effects of incorporating hysteresis on local magnetic fields and iron losses and global results, such as currents, voltages, force/torque, and transients for a wide range of electromagnetic devices. The comparison with the conventional SV model will also be presented.

## 1. The single sheet tester (SST) [4]

The magnetic properties of steels are measured in the laboratory using steel strips (dimension: 30 mm x 250 mm x 0.35 mm) in magnetic testers, e.g., a single sheet tester (SST), an Epstein frame, etc. The first application example is the single SST sample itself. The Simcenter MAGNET model of the SST sample is shown in figure 3 (a). An excitation coil surrounds the sample, and the voltage in the coil can be tuned to get the desired flux density B in the sample.

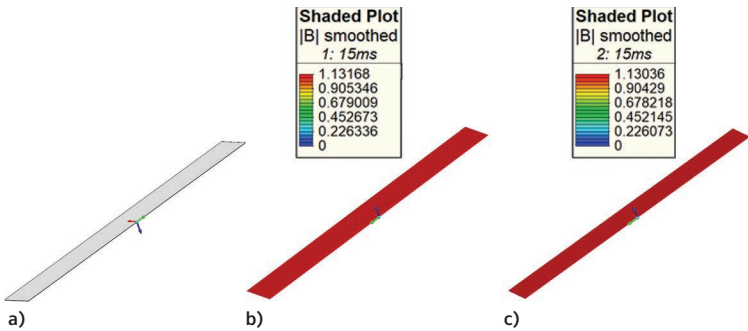


Figure3: Simulation Model of a single strip of 35WW300 non-oriented electrical steel (a) Solid view, uniform B field computed using the (b) single-valued (SV) model, and the (c) hysteresis (Hys) model at 15 milliseconds (peak of the sinusoidal excitation).

The model is solved using both the SV and the Hys models for 35WW300 non-oriented electrical steel. The B field plots using both models are shown in figures 3 (b) and (c) at t = 15 ms. In the case of the SV model, the iron losses are calculated in the post-processing stage using the empirical loss formula in Simcenter MAGNET, given below.

$$(3) \quad P_{IronLoss} = K_{hys} f B^{\alpha} + K_{eddy} f^2 B^2$$

Where,  $K_{hys}$ ,  $\alpha$  and  $K_{eddy}$  are the material loss coefficients which are identified using the power loss curves provided by the user. When using the Hys model, hysteresis loss term in (3), i.e.,  $K_{hys} f B^{\alpha}$  is replaced by (4) which computes the area of the BH loop.

$$(4) \quad P_{HysteresisLoss} = \frac{1}{T} \int_0^T H \cdot \frac{dB}{dt} dt$$

The computed coil currents corresponding to  $B_{max} = 1.13$  T in the sample using the two models are shown in figure 4 (a). A comparison of the measured and computed BH loops (using the Hys model) is presented in figure 4 (b) to reflect the accuracy of the Hys model. A sinusoidal voltage of different amplitudes was applied to calculate the iron loss at different induction levels using both the SV and Hys models, and the results are shown in figure 5.

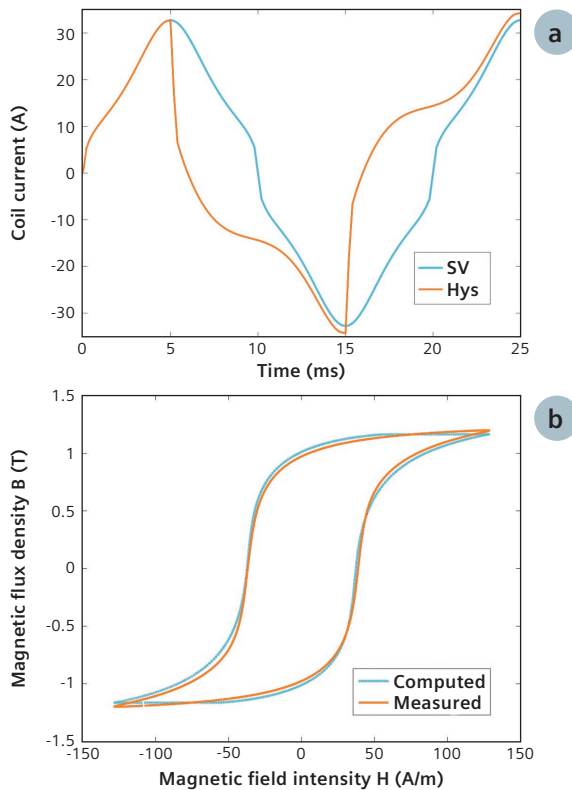


Figure 4: (a) Coil Current computed using the SV and the Hys models at  $B_{max} = 1.13$  T (b) computed and measured BH loops at  $B_{max} = 1.13$  T

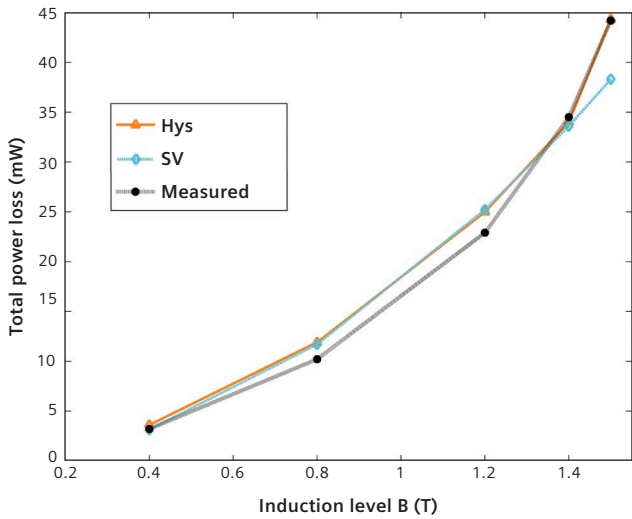


Figure 5: Measured and computed iron losses using the SV and the Hys models. The frequency is 50 Hz.

Stored magnetic energies computed by Simcenter MAGNET for the SST sample using both the SV and Hys models are shown in figure 6. As explained earlier, the hysteresis loss calculation using the Hys model also includes the stored magnetic energy which keeps accumulating over time. For this reason, magnetic stored energy in Simcenter MAGNET v7.9 is disabled for the Hys case. However, the hysteresis loss is not incorporated in the field solutions when using the SV model and the stored magnetic energy can be computed directly from the SV curve.

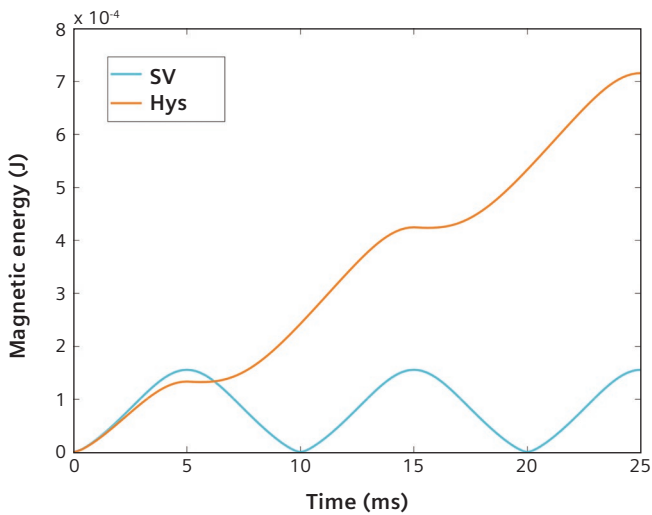


Figure 6: Stored magnetic energy. In the case of the Hys model, it represents the energy being dissipated as hysteresis loss which keeps increasing over time.

Table 1 shows the power balance using both models for one complete cycle of the excitation. It can be seen that the time-averaged stored magnetic energy is zero for the SV case. However, time-averaged stored magnetic energy (hysteresis loss) is a part of the power balance equation. The small difference arising in both cases is due to the numerical integration error and can be ignored.

Table 1 – Power balance (one excitation cycle, frequency = 50 Hz)

Model used	SV	Hys
Average input power (IV) (W)	$9.7 \times 10^{-7}$	0.148719
Time-averaged stored magnetic energy (W)	0	0.148756
Time-averaged Ohmic loss (W)	$3.21 \times 10^{-7}$	$2.48 \times 10^{-7}$
Difference	$6.39 \times 10^{-7}$	$3.21 \times 10^{-5}$

## 2. Team 32 problem [5]

The test bench is a three-limbed ferromagnetic core, as shown in figure 7 (a). The core is made of five Fe-Si 3.2% wt, 0.48 mm thick laminations, having a conductivity  $\sigma = 1.78 \text{ MS/m}$  and a mass density  $\delta = 7650 \text{ kg/m}^3$ . Two windings of 90 turns are placed on the external limbs; the DC resistance of each winding is of 0.32 ohms. These windings can be both connected in series or supplied by two independently controlled voltage sources.

Here we will only consider the case where the two windings are excited by two independent sinusoidal sources with an amplitude of 14.5 V, 10 Hz frequency and differing by  $90^\circ$  in phase. In this way, we will have a rotation of fields in the upper part of the central limb of the device (at point P in figure 7 (a)).

The Simcenter MAGNET model of the problem is shown in figure 7(b). The simulation was run for 125 milliseconds (for 1.25 periods of excitation with 40 points per period) using both the SV and the Hys models. The shaded plots for computed B fields at  $t = 75 \text{ ms}$  using both models are shown in figure 8 (a) and (b), respectively. It can be seen that for the Hys case (shown in figure 8 (b)) almost no flux lines are present in the rightmost limb and flux lines are closing on themselves at the corners of the same limb. The arrow plots for both B and H fields are shown in figures 9 and 10, respectively to investigate this phenomenon. It can be

seen that H field varies between 0 A/m (outer corner) to almost 100 A/m (inner corners) on the rightmost limb. In the SV case shown in figures 9(a) and 10 (a), the sign of B changes with H, i.e., the SV BH curve passes through origin ( $H = 0, B = 0$ ). However in the Hys case, the ferromagnetic material has coercivity, and B reversal happens when H reaches the coercivity thus the field nodes have different signs of B in the same corner, i.e., although H does not change sign B does.

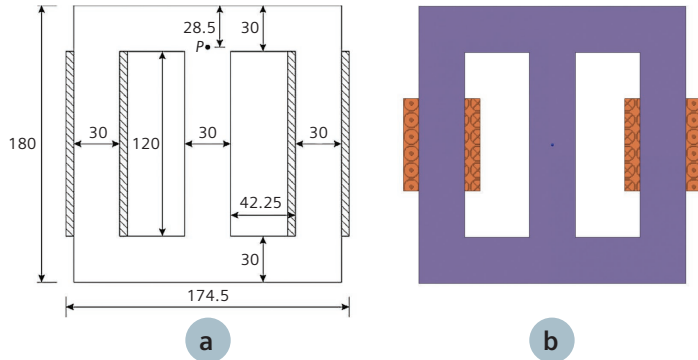


Figure 7: (a) Geometry of the 3 limb transformer [6] (dimension in mm) (b) Simcenter MAGNET Model.

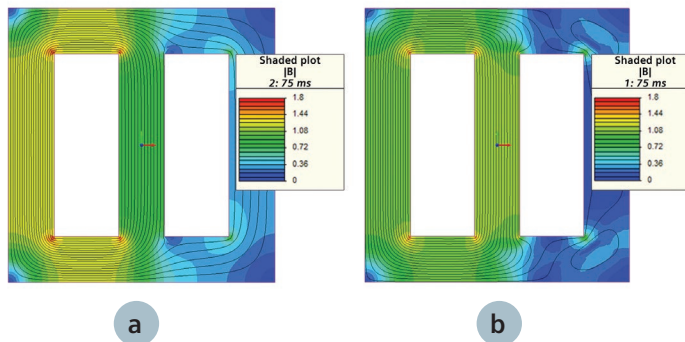


Figure 8: B field shaded plot at  $t = 75$  ms computed using the (a) SV, and the (b) Hys models.

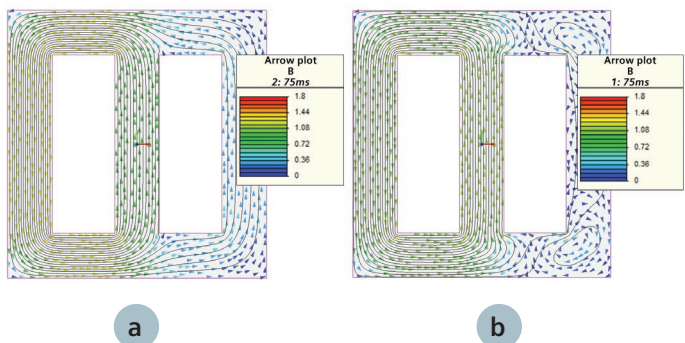


Figure 9: B field arrow plot at  $t = 75$  ms computed using the (a) SV, and the (b) Hys models.

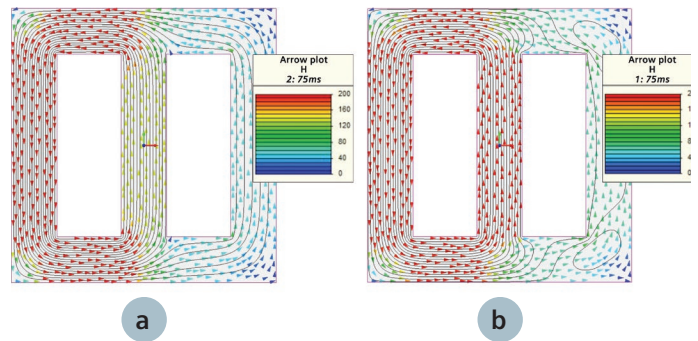


Figure 10: H field arrow plot at  $t = 75$  ms computed using the (a) SV, and the (b) Hys models.

The voltages and flux linkages of both coils using both material models are shown in figure 11 (a) and (b), respectively. The phase difference in the Hys case is obvious because of the phase lag between B and H fields. The results for computed and measured coil currents and magnetic flux densities at point P are shown in figure 12 (a) and (b), respectively. The results for the first quarter of the excitations are not shown because of the initial magnetization curve. A good agreement is achieved when using the Hys model which makes a good case for its use in electromagnetic simulations.

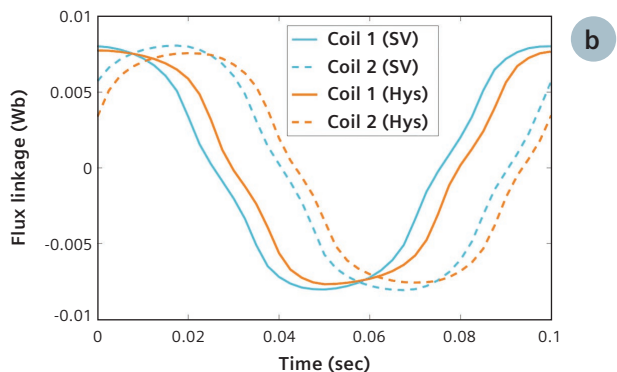
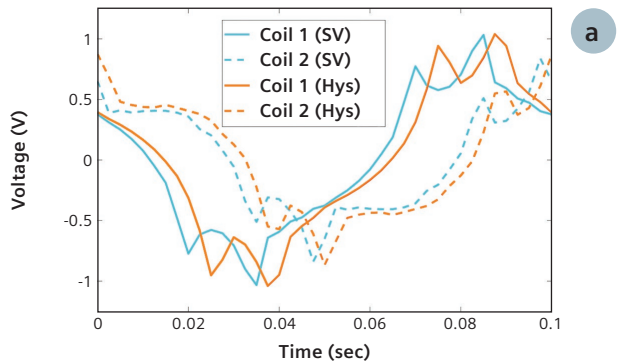


Figure 11: (a) Voltages across two coils and (b) flux linkages in two coils using the SV and the Hys models.

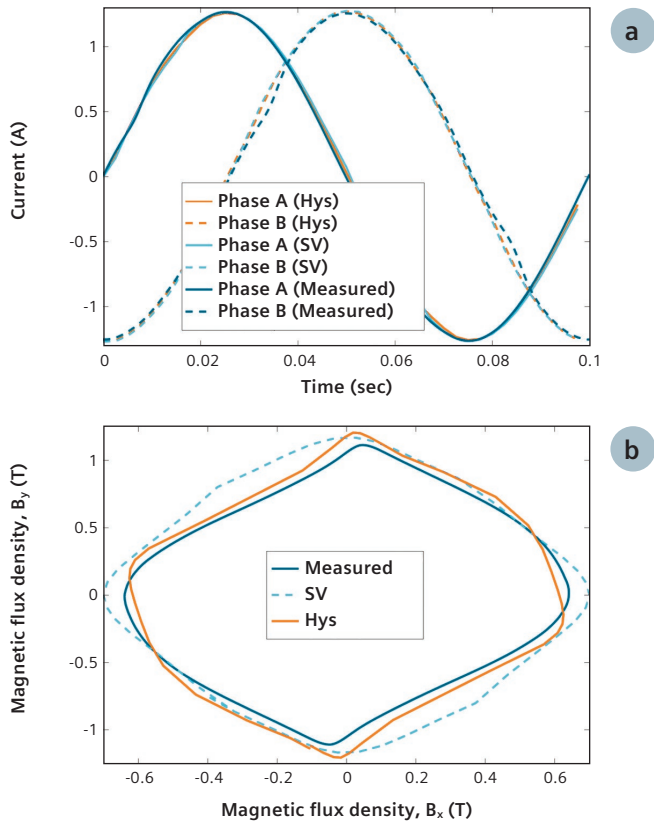


Figure 12: Computed and measured (a) Coil Currents, and (b) B<sub>x</sub> and B<sub>y</sub> flux densities at point P.

### 3. An actuator

In this example, a load-driven electromagnetic actuator is simulated using the Transient 2D with motion solver in Simcenter MAGNET. The simulation model of the actuator is shown in figure 13 (a). The coil in the actuator is driven by a capacitor charged to 12 V. A spring holds the plunger against the upper stop. At time t=0, a switch closes to connect the charged capacitor to the coil. Both the body and plunger are made with M47 – 24 Ga steel.

The shaded plot for the computed B fields at t = 26.9 ms for the SV and the Hys models are shown in figures 13 (a) and 13 (b), respectively. There is not much noticeable difference here. However, it is desired to accurately predict the position of the plunger as a function of time. Figure 14 (a) illustrates the difference between computed positions as a function of time using both models and a lag between the SV and the Hys case can be observed. This can be important for critical applications where accurate knowledge of the position is desired. The coil currents computed using both models are also shown in figure 14 (b).

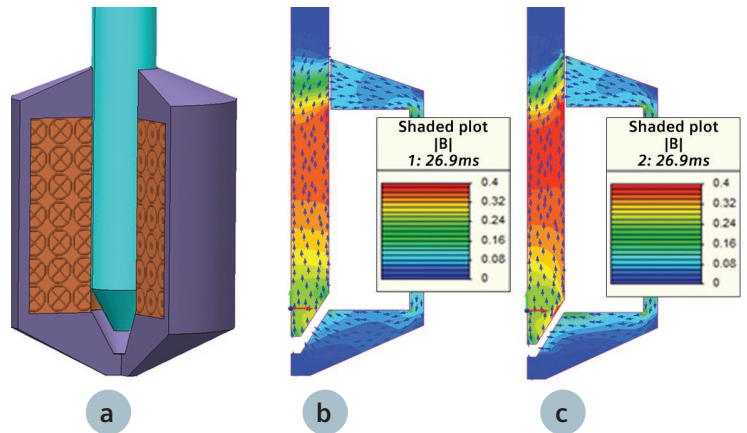


Figure 13: (a) Simcenter MAGNET model of an actuator. B field shaded, and arrow plot at t = 26.9 ms computed using the (b) SV, and the (c) Hys models

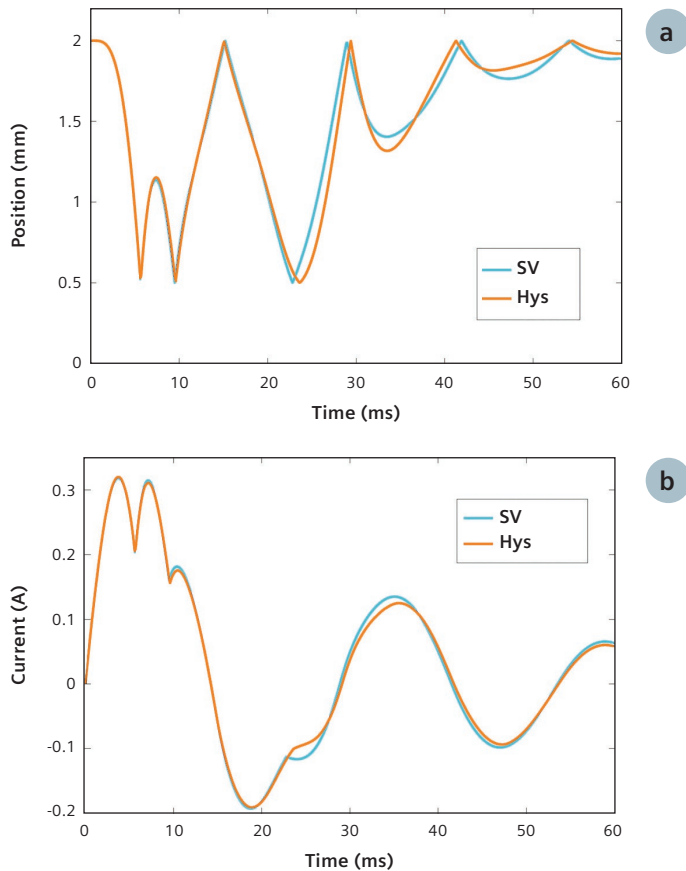


Figure 14: (a) Position of the actuator and (b) Excitation coil current computed using the SV and the Hys models.

#### 4. An induction machine [6]

A Simcenter MAGNET simulation of a voltage-driven induction motor is presented here. The rated specifications of the test motor are provided in table 2.

The full Simcenter MAGNET model of the unskewed motor is shown in figure 15. For simulation purposes, the quarter model was solved for 25 supply cycles (frequency = 50 Hz) using the 2D Transient solver with motion. Shaded plots for computed B fields at t = 500 ms are shown in figure 16 for both the SV and the Hys models. The difference in rotor position at 500 ms for both models can be noticed.

Table 2 – Induction machine specifications

Rated power	11 kW
Rated torque	70 N.m
Rated voltage	400 Volts
Frequency	50 Hz
Number of poles	4
Number of slots	36
Number of rotor bars	28
Slip	~ 1 %
Stator and rotor core material	M-19 29 Ga Steel

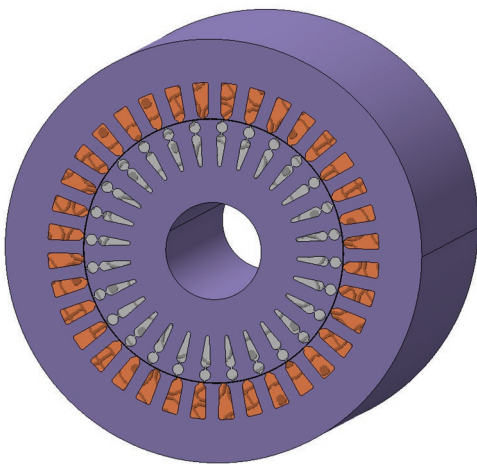


Figure 15: Simcenter MAGNET model of 36 slots, 28 bars, 4 poles induction machine.

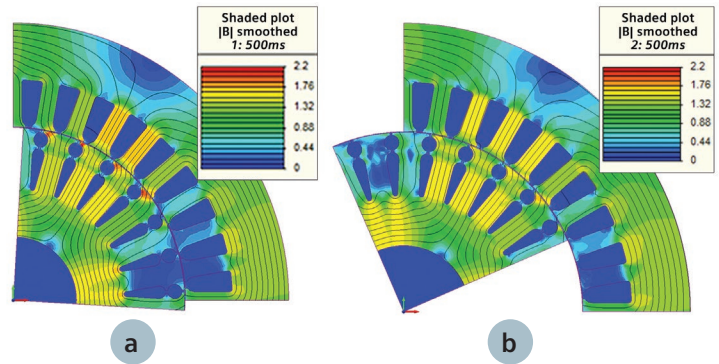


Figure 16: B field shaded plot at t = 500 ms computed using the (a) SV, and the (b) Hys models.

The flux linkages and currents of phase A are shown in figures 17 (a) and (b), respectively. It can be seen that there is a transient in the solution. The Hys model predicts higher overshoots in the current waveform, but the transients die out faster than the SV model because of the energy dissipation in the ferromagnetic material changing the time constant of the system. This also implies that steady state is achieved earlier and hysteresis simulations can be run for a lower number of time steps in this case. An induction machine is a rotating transformer. Therefore, similar results can be expected in transformer simulations.

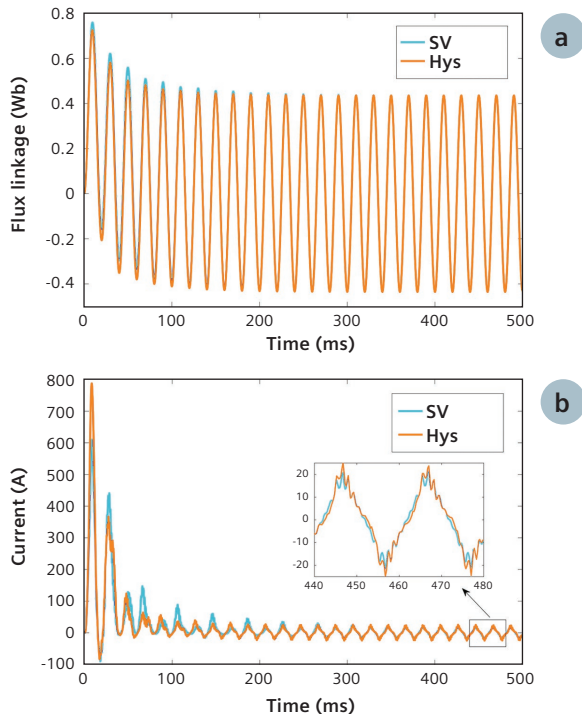


Figure 17: (a) Flux linkage and (b) Phase current of phase A computed using the SV, and the Hys models.

The speed and torque characteristics of the induction machine are shown in figures 18 (a) and (b), respectively and similar transient behaviour is observed. There is no significant difference in values at the steady state. Figure 19 presents the time-averaged power losses (hysteresis loss, eddy current loss and ohmic loss) in various parts of the machine. The hysteresis loss in the rotor is not presented here because the slip frequency, 0.5 Hz in this case, is very small and obtaining time-averaged hysteresis loss for one complete cycle of rotor frequency in the Hys case will take too many solution steps.

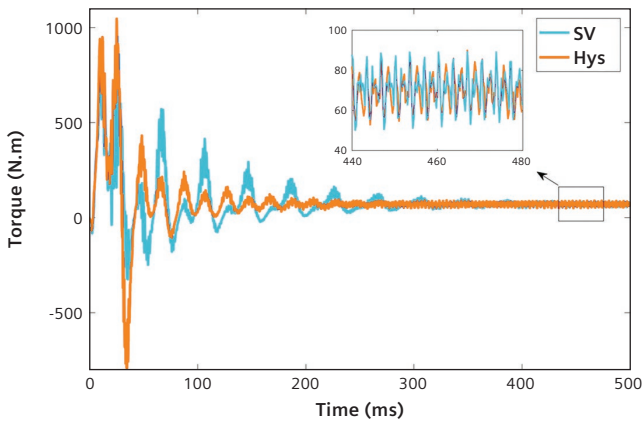
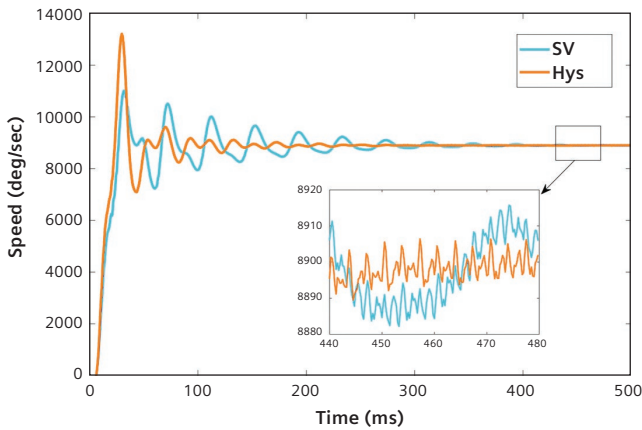


Figure 18: (a) Speed and (b) Torque computed using the SV, and the Hys models.

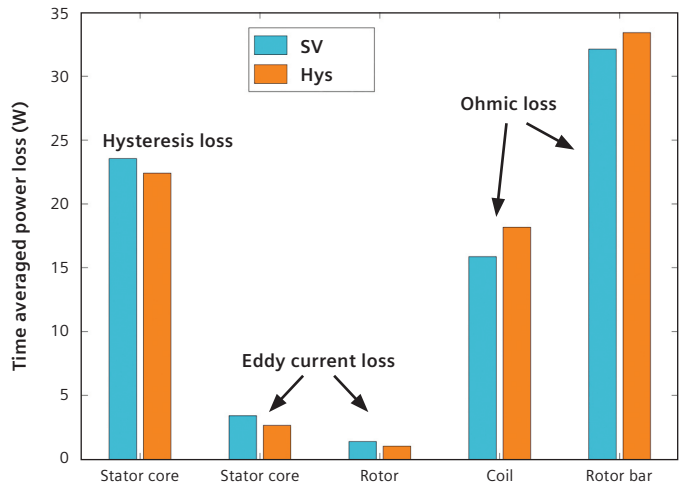


Figure 19: Power loss in different parts of the machine computed using the SV, and the Hys models.

### 5. A surface mounted permanent magnet fractional slot internal rotor machine [7]

This example illustrates the current-driven simulation of a surface-mounted permanent magnet (SMPM) fractional slot, concentrated winding, synchronous machine which is used for traction applications. The specifications of the motor are shown in table 3.

Table 3 – SMPM machine specifications

Rated power	30 kW
Rated torque	120 N.m
Rated max current	200 A
Base speed	2800 RPM
Frequency	233.33 Hz
Number of poles	10
Number of slots	12
Stator and rotor material	M-19 29 Ga Steel

The full Simcenter MAGNET model of the SMPM synchronous machine is shown in figure 20 and was solved in the low-speed (frequency = 50 Hz) high-torque region for five supply cycles using the 2D Transient with motion solver. Shaded plots for the computed B fields at  $t = 0$  ms using the SV and the Hys models are shown in figures 21 (a) and (b), respectively. It can be seen that the stator teeth are in deep saturation (around 2 T) in the SV case which means that the extrapolation of the SV BH curve overestimates the field values.

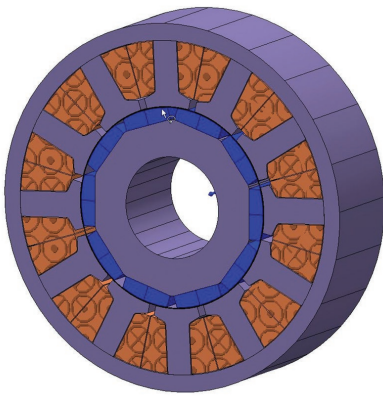


Figure 20: Simcenter MAGNET model of a 12 slots 10 poles surface mounted PM fractional slot machine.

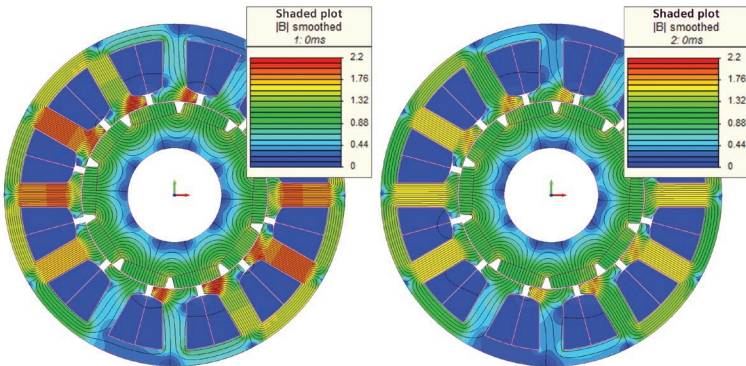


Figure 21: B field shaded plot at  $t = 0$  ms computed using the (a) SV, and the (b) Hys models.

The flux linkages and voltages of phase A computed using the SV and the Hys models are shown in figures 22 (a) and (b), respectively. The flux linkage in the Hys case is smaller than the SV case, and the effects of the slots on the voltage can be seen when using the Hys model. The computed torque using both material models is shown in figure 23. Since iron losses are incorporated into the field solution in the case of the Hys model; the resulting torque is less than that of the SV model. Iron losses computed using both models are not very different and are shown in figure 24.

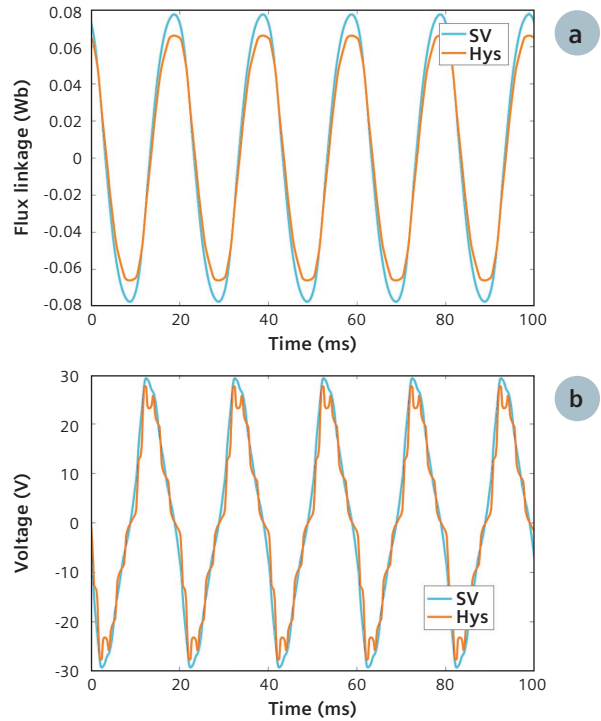


Figure 22: (a) Flux linkage and (b) Phase voltage of Phase A computed using the SV and the Hys models.

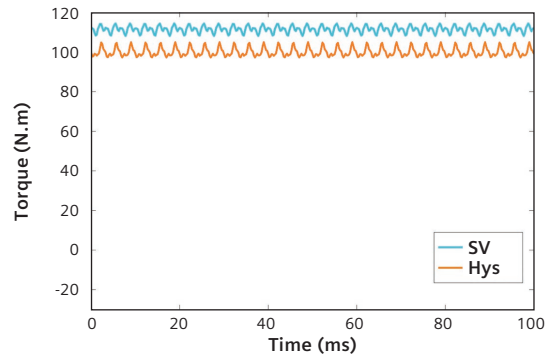


Figure 23: Torque computed using the SV and the Hys models.

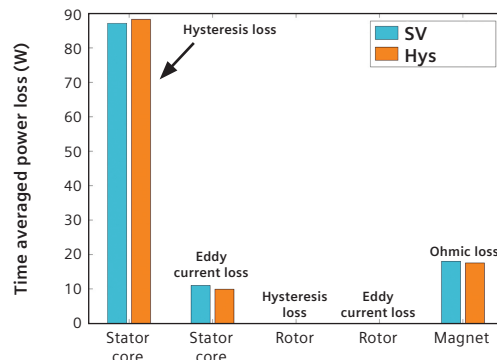


Figure 24: Power loss in different parts of the machines computed using the SV and the Hys models.

# Time performance

The time performance of the Hys model is important for users. A solution which takes too much computation time is not generally desirable for the design engineers. Therefore, the total simulation times for solving the examples mentioned above using both the SV and the Hys model are shown in table 4, and their ratio is plotted in figure 25.

It is important to note that this plot provides an estimation of time performance of the Hys model compared to the SV model and can vary a lot depending on the number of time steps per cycle, mesh density, polynomial order, etc. The solver settings used for collecting the data given in table 4 are time steps per cycle = 100, polynomial order = 2, Newton tolerance = 1 percent. Lowering the Newton tolerance to very small values increases the number of nonlinear iterations which significantly increases the simulation times.

**Table 4 – Simulation time ratio of the SV and the Hys models**

Simulation model	Ratio ( $T_{\text{Hysteresis}} / T_{\text{Single-Valued}}$ )
SST sample	2.56
TEAM 32	1.85
Actuator	3.79

Simulation model	Ratio ( $T_{\text{Hysteresis}} / T_{\text{Single-Valued}}$ )
Induction machine	2.94
Surface mounted permanent magnet (SMPM)	1.27
Fractional slot internal rotor machine	

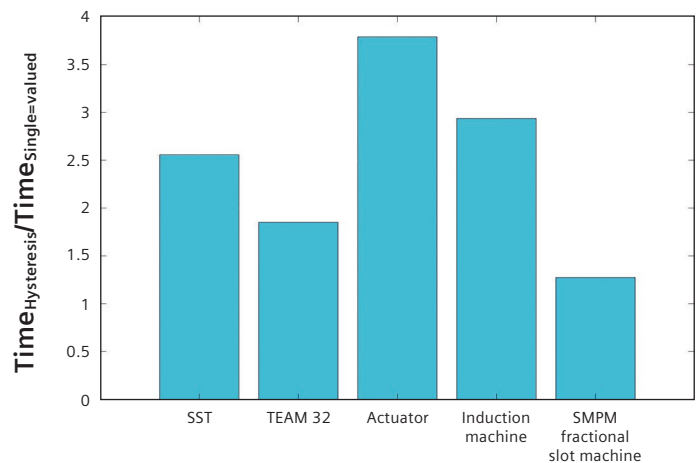


Figure 25: Time performance of the Hys model compared to the SV model.

## References

1. D. C. Jiles and D. L. Atherton. "Theory of ferromagnetic hysteresis", *J. Magn. Magn. Mater.*, vol. 61, no. 1–2, pp. 48–60, 1986.
2. F. Preisach. "Über die magnetische Nachwirkung", *Zeitschrift für Phys.*, vol. 94, no. 5–6, pp. 277–302, 1935.
3. A. J. Bergqvist. "A simple vector generalization of the Jiles-Atherton model of hysteresis", *IEEE Trans. Magn.*, vol. 32, no. 5 PART 1, pp. 4213–4215, 1996.
4. S. Hussain, Development of advanced material models for the simulation of low-frequency electromagnetic devices, Ph.D. Thesis, McGill University, Montreal, Canada, Feb. 2017.
5. O. Bottauscio, M. Chiampi, C. Ragusa, L. Rege, and M. Repetto. "Description of TEAM Problem: 32 A test case for validation of magnetic field analysis with vector hysteresis", 2010. [Available online] [www.compumag.org/j/site/images/stories/TEAM/problem32.pdf](http://www.compumag.org/j/site/images/stories/TEAM/problem32.pdf)
6. S. Hussain, V. Ghorbanian, A. Benabou, S. Clénet, D. A. Lowther. "A study of the effects of temperature on magnetic and copper losses in electrical machines", *Proc. 2016 XXII Int. Conf. Elect. Mach.*, pp. 1277–1283, 2016.
7. T. Rahman, R. C. P. Silva, K. Humphries, M. H. Mohammadi, D. A. Lowther. "Design and optimization of fractional slot concentrated winding permanent magnet machines for class IV electric vehicles", *Proc. IEEE Transp. Electrific. Conf. Expo. (ITEC)*, June 2016.

## Siemens Digital Industries Software

### Headquarters

Granite Park One  
5800 Granite Parkway  
Suite 600  
Plano, TX 75024  
USA  
+1 972 987 3000

### Americas

Granite Park One  
5800 Granite Parkway  
Suite 600  
Plano, TX 75024  
USA  
+1 314 264 8499

### Europe

Stephenson House  
Sir William Siemens Square  
Frimley, Camberley  
Surrey, GU16 8QD  
+44 (0) 1276 413200

### Asia-Pacific

Unit 901-902, 9/F  
Tower B, Manulife Financial Centre  
223-231 Wai Yip Street, Kwun Tong  
Kowloon, Hong Kong  
+852 2230 3333

## About Siemens Digital Industries Software

Siemens Digital Industries Software is driving transformation to enable a digital enterprise where engineering, manufacturing and electronics design meet tomorrow. Our solutions help companies of all sizes create and leverage digital twins that provide organizations with new insights, opportunities and levels of automation to drive innovation. For more information on Siemens Digital Industries Software products and services, visit [siemens.com/software](https://www.siemens.com/software) or follow us on [LinkedIn](#), [Twitter](#), [Facebook](#) and [Instagram](#). Siemens Digital Industries Software – Where today meets tomorrow.

[siemens.com/software](https://www.siemens.com/software)